Insight into the evolution and origin of leprosy bacilli from the genome sequence of *Mycobacterium lepromatosis*

Pushpendra Singh[a,1,2], Andrej Benjak[a,1], Verena J. Schuenemann[b], Alexander Herbig[b], Charlotte Avanzi[a], Philippe Busso[a], Kay Nieselt[c], Johannes Krause[b,d,e], Lucio Vera-Cabrera[f], and Stewart T. Cole[a,3]

[a]Global Health Institute, Ecole Polytechnique Fédérale de Lausanne, 1015 Lausanne, Switzerland; [b]Institute for Archaeological Sciences, University of Tübingen, 72076 Tübingen, Germany; [c]Center for Bioinformatics Tübingen, University of Tübingen, 72070 Tübingen, Germany; [d]Senckenberg Centre for Human Evolution and Palaeoenvironment, University of Tübingen, 72070 Tübingen, Germany; [e]Max Planck Institute for the Science of Human History, 07745 Jena, Germany; and [f]Laboratorio Interdisciplinario de Investigación Dermatológica, Servicio de Dermatología, Hospital Universitario, Universidad Autónoma de Nuevo León, 64460 Monterrey, Nuevo León, Mexico

Mycobacterium lepromatosis is an uncultured human pathogen associated with diffuse lepromatous leprosy and a reactional state known as Lucio's phenomenon. By using deep sequencing with and without DNA enrichment, we obtained the near-complete genome sequence of *M. lepromatosis* present in a skin biopsy from a Mexican patient, and compared it with that of *Mycobacterium leprae*, which has undergone extensive reductive evolution. The genomes display extensive synteny and are similar in size (~3.27 Mb). Protein-coding genes share 93% nucleotide sequence identity, whereas pseudogenes are only 82% identical. The events that led to pseudogenization of 50% of the genome likely occurred before divergence from their most recent common ancestor (MRCA), and both *M. lepromatosis* and *M. leprae* have since accumulated new pseudogenes or acquired specific deletions. Functional comparisons suggest that *M. lepromatosis* has lost several enzymes required for amino acid synthesis whereas *M. leprae* has a defective heme pathway. *M. lepromatosis* has retained all functions required to infect the Schwann cells of the peripheral nervous system and therefore may also be neuropathogenic. A phylogeographic survey of 227 leprosy biopsies by differential PCR revealed that 221 contained *M. leprae* whereas only six, all from Mexico, harbored *M. lepromatosis*. Phylogenetic comparisons indicate that *M. lepromatosis* is closer than *M. leprae* to the MRCA, and a Bayesian dating analysis suggests that they diverged from their MRCA approximately 13.9 Mya. Thus, despite their ancient separation, the two leprosy bacilli are remarkably conserved and still cause similar pathologic conditions.

Mycobacterium lepromatosis | genome sequencing | *Mycobacterium leprae* | comparative genomics | reductive evolution

Nearly a quarter million new cases of leprosy (Hansen's disease) are still recorded annually worldwide despite a remarkable decrease in prevalence in the past decade (1). Leprosy primarily affects the skin, peripheral nerves, and eyes, and manifests as a spectrum of diverse clinical forms varying in bacillary load and often accompanied by painful immunological reactions (2–4). A severe form of leprosy known as diffuse lepromatous leprosy (DLL) that is common in western Mexico and the Caribbean region, first described by Lucio and Alvarado in 1852 (5), is referred to as Lucio's leprosy. Such cases account for a sizable proportion (more than 20%) of all leprosy cases in western Mexico (5–8), Cuba (9), and Costa Rica (10) but are rarely reported elsewhere. In 1948, Latapi and Zamora noted that DLL cases had no dermal nodules and were characterized by a generalized and diffuse infiltration of the skin by histiocytes and acid-fast bacilli causing an appearance of swollen or "spotted" skin, which they termed "pure and primitive diffuse lepromatosis." In addition, they reported that some patients developed acute necrotic skin reactions, "erythema necroticans," and differentiated

this condition as Lucio's phenomenon (6). The most notable clinical feature of DLL and Lucio's phenomenon is the diffuse mycobacterial invasion of endothelial cells surrounding small vessels, often leading to vascular occlusion (8). The initial cyanotic lesions, caused by poor blood supply and ischemia, gradually evolve into black necrotic lesions (11, 12). Hence, these cases are often associated with long-term morbidity (8) as well as a higher number of fatalities if not managed adequately (5, 13).

Lucio's phenomenon is usually observed among untreated or inadequately treated nonnodular DLL cases 1–3 y after the appearance of their symptoms. Although rare, Lucio's phenomenon has also been reported among other forms of lepromatous leprosy (6). Multidrug therapy (MDT) is currently the treatment recommended by the World Health Organization for all forms of leprosy, including DLL and Lucio's phenomenon (14, 15). Until recently, *Mycobacterium leprae* was considered the sole causative agent of all forms of leprosy, including Lucio's phenomenon,

Significance

Leprosy was thought to be exclusively caused by infection of humans by *Mycobacterium leprae*. In 2008, Han et al. proposed that *Mycobacterium lepromatosis*, a separate unculturable species, might be responsible for a rare yet severe form of the disease called diffuse lepromatous leprosy. Here, by using comparative genomics, we show that the two species are very closely related and derived from a common ancestor that underwent genome downsizing and gene decay. Since their separation 13.9 Mya, the two species have continued to lose genes, but from different regions of the genome, and *M. leprae* appears to be more recent. In a phylogeographic survey, by using differential PCR, we found that *M. lepromatosis* was scarce and restricted to patients from Mexico.

MICROBIOLOGY

which is often referred to as a "form of leprosy reaction" (13, 16). The genome of *M. leprae* has undergone reductive evolution, with approximately half occupied by pseudogenes (17), and also displays remarkably low levels of genetic diversity (18–20).

In 2008, a new mycobacterial species named *Mycobacterium lepromatosis* was identified in a liver autopsy specimen from a homeless Mexican who died with DLL in Arizona (21). Since then, this species has been identified by PCR-based sequencing in several Mexican patients (22) as well as in individual cases from Singapore (23) and Canada (24). In addition, clinical presentations resembling Lucio's phenomenon have been reported elsewhere, i.e., Brazil (25, 26), India (27–29), Iran (30), and Malaysia (31); however, molecular confirmation of the mycobacterial agent was not carried out. In addition, several cases of mixed infection have been reported whereby both *M. lepromatosis* and *M. leprae* were detected (22), which undermines confidence in *M. lepromatosis* being the causative agent of DLL.

Knowledge about the biology and pathogenesis of *M. lepromatosis* is limited because this species remains uncultivated (21). To date, the DNA sequences of 22.8 kb of selected PCR fragments from *M. lepromatosis* are known, and these were sufficient to reveal striking sequence similarity to *M. leprae* and a close phylogenetic relationship, but this preliminary analysis provided little biological insight. Thus, at this stage, genome sequencing is the most efficient approach to investigate *M. lepromatosis*.

After the first description of *M. lepromatosis* by Han et al. in 2008 (21), we reported independent confirmation of this species in a biopsy specimen from a DLL case (Mx1-22A) from Monterrey, Mexico (32). Here, we combined various DNA enrichment approaches and deep sequencing to unveil the genome of *M. lepromatosis* directly from the archived biopsy specimen from this patient. Genome-wide comparison of *M. lepromatosis* and *M. leprae* provides deeper insight into the biology of *M. lepromatosis* and discloses the evolutionary history of these two closely related but clearly distinct species.
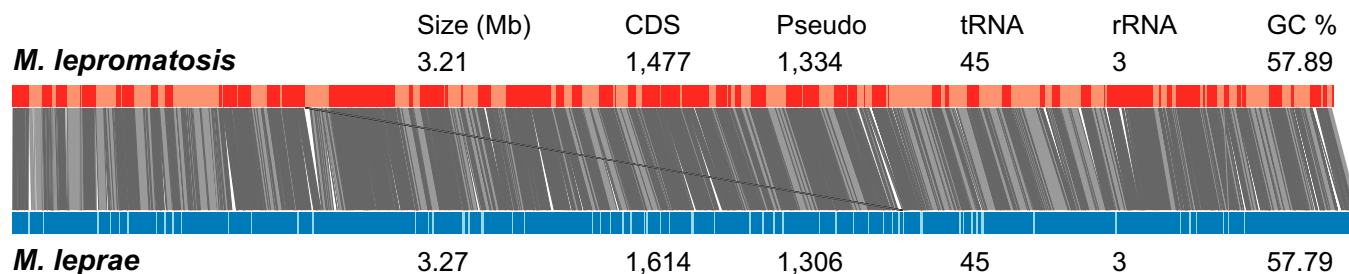
Results and Discussion

Genome Sequencing, Assembly, and Analysis. Because *M. lepromatosis* cannot be cultured in vitro and an animal model is not yet available, the only source of its DNA is infected human tissue. Biopsy specimen Mx1-22A was used for DNA extraction and Illumina library preparation as described previously (20). To overcome the problem of host DNA, we used two methods to enrich *M. lepromatosis* DNA: whole-genome array capture using the *M. leprae* genome as bait (20) and removal of human DNA by hybridization with a human genomic DNA bait library (*Materials and Methods*). Illumina sequencing of the enriched as well as the original libraries provided 55-fold coverage, which was more than sufficient for the de novo whole-genome assembly (Table S1).

The genome assembly was obtained by relaxing the assembler program's parameters (*Materials and Methods*) to account for the extremely biased read coverage from the array capture library. Contigs were considerably longer compared with those obtained with default assembly parameters, but at the cost of a higher chance of misassemblies. To avoid assembly errors, we split those contigs showing disrupted synteny with *M. leprae* so that, from the initial 110 contigs of the de novo assembly, we obtained a final set of 126 contigs. Most inconsistencies in the contigs were observed around areas of repetitive DNA, with some exceptions. One such exception was confirmed by PCR sequencing (as detailed later), proving that there is at least one instance of genome rearrangement between *M. leprae* and *M. lepromatosis*. However, we consider that the overall level of rearrangement is low, given that only a few contigs showed breaks in synteny with the reference genome and the GC skew of the "syntenic" version of the *M. lepromatosis* genome is virtually identical to that of *M. leprae* (Fig. S1).

A total of 3,206,741 bases of the *M. lepromatosis* Mx1-22A genome were represented in the 126 contigs, and, with one exception, these all aligned to the 3.27-Mb circular genome sequence of the Tamil Nadu (TN) reference strain of *M. leprae* (17). The exception was a 2.3-kb contig bearing five mycobacterial pseudogenes. A graphical comparison revealing genome-wide synteny and key features of the two genomes is presented in Fig. 1. In brief, the genome of *M. lepromatosis* appears to harbor at least 1,477 genes encoding proteins [i.e., coding DNA sequence (CDS)] and 1,334 pseudogenes.

Repetitive DNA. Dispersed repeats were the major cause of breaks in our de novo assembly. Interestingly, in most cases, the locations of these repeats correspond to those of the four main families of repetitive DNA in *M. leprae*: RLEP (37 copies), REPLEP (15 copies), LEPREP (8 copies), and LEPRPT (5 copies) (33). These shared 75–90% sequence identity, in segments as much as 350 nt in length, with the most conserved corresponding to LEPREP and LEPRPT repeats and the lowest homology found for the REPLEP repeats. From this analysis, it is evident that the four repeat families were present in the most recent common ancestor (MRCA) of *M. leprae* and *M. lepromatosis* and that the levels of conservation between the repeats in the two species are proportional to their copy number. No additional repetitive DNA was detected in *M. lepromatosis*.

A Second Draft Genome. Using the *M. lepromatosis* genome sequence, we designed specific PCR primers and used them to screen ~260 biopsies from our collection, thereby identifying a second case of *M. lepromatosis* in another Mexican patient (Mx177) who presented with Lucio's phenomenon. This sample, which contained no *M. leprae* DNA, was shotgun-sequenced, without any enrichment, and the resultant sequences were mapped against the Mx1-22A genome assembly. Despite shallow coverage of the Mx177

	Size (Mb)	CDS	Pseudo	tRNA	rRNA	GC %
M. lepromatosis	3.21	1,477	1,334	45	3	57.89
M. leprae	3.27	1,614	1,306	45	3	57.79

Fig. 1. Genome synteny and salient features of *M. leprae* and *M. lepromatosis*. The 126 contigs of *M. lepromatosis* are distinguished with red and orange colors. Links between *M. leprae and M. lepromatosis* are BLAST hits, with two shades of gray to distinguish individual contigs. White stripes indicate no BLAST hits and account for 5–6% of each genome's specific sequences. Light blue stripes indicate dispersed repeats in *M. leprae*. Black line indicates a confirmed structural variation between *M. leprae* and *M. lepromatosis*.
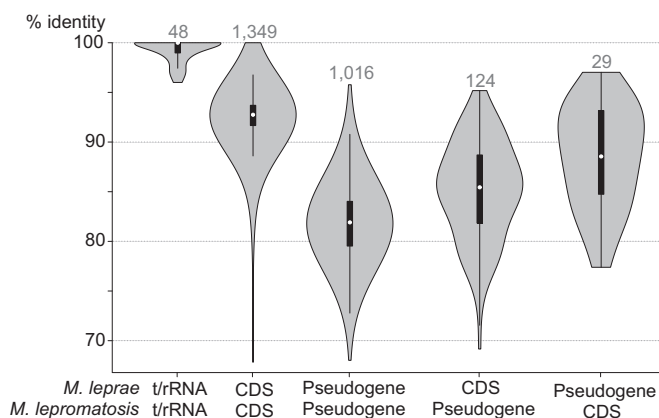
sample (80% of the genome at an average coverage of 5× after excluding duplicate reads), we found only 12 SNPs in a 2-Mb alignment where SNP calling was feasible. This very low SNP frequency (1 in 167 kb) is reminiscent of the similarly low genetic diversity of *M. leprae* strains from the same geographical area (34) and in a set of worldwide *M. leprae* genomes in general (20).

Synteny and Conservation of the *M. lepromatosis* and *M. leprae* Genomes. Ninety-four percent of the *M. lepromatosis* genome assembly could be aligned to the *M. leprae* TN genome, and there appears to be near-perfect collinearity and synteny, with 92% of the genes and pseudogenes shared (Fig. 1). Details of (pseudo)genes that have been deleted are provided in Dataset S1. In *M. leprae*, there are tandemly arranged asparagine permease genes (*ML1304c ML1305c*; *ansP1 ansP2*), but only one of these is present in *M. lepromatosis* (*MLPM_1304*). Likewise, a duplicated cluster of four genes in *M. leprae* (*ML1053-ML1056*; *ML1180c-ML1183c*) is present as a single copy in *M. lepromatosis* (*MLPM_1053-MLPM_1056*). This cluster encodes a member of the PE- and PPE-protein families and the ESAT-6 proteins, EsxL and EsxK.

M. lepromatosis has intact orthologs for 95% of the CDS present in *M. leprae*, but a further 132 CDS appear to have been pseudogenized in *M. lepromatosis* (Table S2). It is noteworthy that four of them (*ilvX, proA, cysE, cysK*) once encoded enzymes required for amino acid biosynthesis. Twenty-six *M. leprae* pseudogenes appear to have functional counterparts in *M. lepromatosis* (Table S3).

Levels of nucleotide sequence conservation for orthologous CDS and pseudogenes from *M. lepromatosis* and *M. leprae* varied between the functional categories, as may be seen from the violin plot (Fig. 2). The most conserved genes code for the rRNA and tRNA (sequence identity >95%), whereas the least conserved were those for the PE/PPE proteins, as these display the hallmarks of selective pressure (as detailed later). On average, CDS shared 93% nucleotide sequence identity between the two species, but this value was only 82% for the pseudogenes. A wide distribution of sequence conservation was seen among pseudogenes (Fig. 2), and this may reflect their respective dates of pseudogenization, as older pseudogenes will have had longer to diverge.

Species-Specific Sequences in *M. lepromatosis* and *M. leprae*. We identified 84 genomic regions of *M. lepromatosis* larger than 500 nt that have no counterparts in *M. leprae*, accounting for a total of 166 kb, or ~5% of the genome. These regions (range, 0.5–9.6 kb

in size) consist essentially of pseudogenes ($n = 163$) except for three intact coding sequences: a hypothetical gene (*MLPM_5094*), a putative lipoprotein gene (*MLPM_5098*), and coproporphyrinogen III oxidase (*hemN*) (discussed later). Truncated remnants of 57 of these 163 pseudogenes remain in *M. leprae*, revealing that some of the reductive evolution in this leprosy bacillus stemmed from deletions within, or encompassing, pseudogenes since divergence from the MRCA.
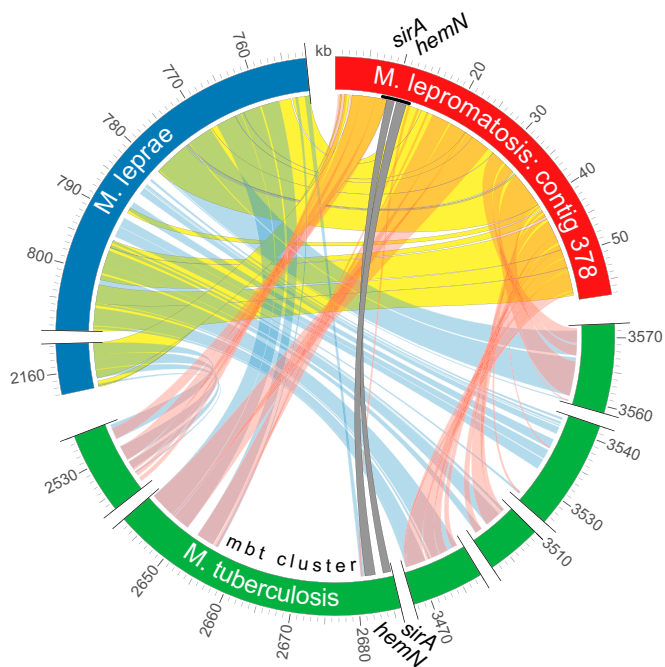
Similarly, *M. leprae* has a total of 199 kb of sequences (>500 nt) in its genome with no counterpart in *M. lepromatosis*. These comprise 172 pseudogenes, of which 54 were partially present in *M. lepromatosis*, and 24 protein-coding genes, all annotated as encoding hypothetical or conserved hypothetical proteins, except for *ML0398c* (possible D-ribose–binding protein), which is truncated in *M. lepromatosis*.

Horizontally Acquired Genes. Several *M. leprae* genes have no orthologs in other mycobacteria and appear to have been acquired by horizontal gene transfer. Among those with predicted functions are *proS*, encoding a eukaryotic-like prolyl tRNA synthetase, and *ML2177*, coding for a uridine phosphorylase that shows similarity to insect enzymes. Both genes are conserved in sequence and location in *M. lepromatosis*, indicating that they were present in the MRCA. Likewise, there are two pseudogenes (*MLPM_5100* and *MLPM_5101* encoding a β-lactamase and LysR family transcriptional regulator) in a genomic island restricted to *M. lepromatosis* that appears to have been horizontally acquired by the MRCA and then lost by *M. leprae*.

Insight into Pathogenesis. The higher morbidity and mortality reported to be associated with infection by *M. lepromatosis* and the resulting DLL suggest the presence of new virulence functions possibly borne by plasmids. For example, the pathogenesis of *Mycobacterium ulcerans* has been attributed to the horizontally acquired virulence plasmid encoding the mycolactone toxin (35, 36). However, despite intensive investigation of Illumina sequence reads with no matches in *M. leprae* and database searches, we found no evidence for plasmid or bacteriophage sequences.

To cope with iron limitation, intracellular pathogens often scavenge heme from host tissue or produce and release siderophores, such as mycobactin, to capture iron (37, 38). Both leprosy bacilli have retained the ESX-3 gene cluster that is involved in iron and zinc uptake in *M. tuberculosis*. The mycobactin (*mbt*) gene cluster is essential for the in vivo growth and virulence of *M. tuberculosis* (39, 40), but this cluster is missing from *M. lepromatosis* and *M. leprae*. In *M. tuberculosis*, *hemN* is located downstream of the *mbt* cluster, and, with the *hemABCDEKLYZ* genes, is required for heme biosynthesis. Interestingly, the *hemN* gene is present in *M. lepromatosis* but not in *M. leprae* (Fig. 3), indicating its loss occurred after separation from the MRCA and suggesting that *M. leprae* may be limited for heme production.

Inspection of the genes least conserved between *M. lepromatosis* and *M. leprae* (Fig. 2) revealed that these correspond mainly to members of the PE and PPE protein families, characteristic of pathogenic mycobacteria, and to the ESX (type 7) protein secretion systems. Compared with *M. tuberculosis* and *Mycobacterium marinum*, there are very few PE and PPE proteins in leprosy bacilli. In *M. leprae*, *ML0411* encodes a PPE protein that acts as an immunodominant serine-rich antigen, whereas the neighboring gene, *ML0410*, codes for a PE family protein. Both genes are present in *M. lepromatosis* but have diverged extensively: there is only 68% nucleotide sequence identity between *MLPM_0411* and *ML0411* (note that only half the genes could be aligned) and 73% between *MLPM_0410* and *ML0410*. Interestingly, sequence comparison of *ML0411* in a range of isolates of *M. leprae* of different geographical origin revealed this to be the most polymorphic gene in the genome, with the highest number of nonsynonymous substitutions (20, 41). It appears that the marked

Fig. 2. Nucleotide sequence identity between *M. leprae* and *M. lepromatosis* orthologs. Numbers above violins represent the number of ortholog pairs for that gene category. The most conserved are tRNA and rRNA genes, followed by the CDS. Pseudogenes are the least conserved. Identity of genes that are functional in one species but not in the other is between CDS and pseudogenes.

Fig. 3. Synteny around the *M. lepromatosis* *hemN* locus and comparison with *M. leprae* and *M. tuberculosis*. Links between the genomes are BLAST hits; *hemN* and *sirA* are present in *M. lepromatosis* and *M. tuberculosis* (gray links) but have been deleted in *M. leprae*. The *mbt* cluster, present in *M. tuberculosis*, is deleted in *M. leprae* and *M. lepromatosis*. Scale is in kilobases. Note the genomic rearrangement between *M. lepromatosis* (first 10 kb of the contig) and *M. leprae*. Additionally, the sequence corresponding to the *M. leprae* genome between 780 and 795 kb is almost entirely deleted in *M. lepromatosis*.

divergence in this locus is the consequence of selective pressure imparted by the host's immune system (20).

The ability to invade the endothelium distinguishes *M. lepromatosis* from *M. leprae*. Because we found no evidence for the presence of a novel virulence gene that could account for this phenotype, we examined the gene clusters required to produce the five type 7 ESX secretion systems (T7Ss) for unusual features. Although not essential for growth in vitro, the ESX-1 system is the major virulence determinant in *M. tuberculosis* and *M. marinum*. ESX-1 mediates escape of the bacilli from the phagosome, thus allowing further replication, cytolysis, necrosis, and intercellular spread (42). The EsxA protein, a major substrate of ESX-1, ruptures the phagosomal membrane, thus acting as a principal virulence factor. Despite extensive conservation of the ESX-1 system among other mycobacterial pathogens, several of its genes encoding ESX-1 secreted proteins (Esp, Esx) are missing or nonfunctional in *M. leprae* and *M. lepromatosis*. These include *espE*, *espB*, *espF*, *espG1*, *espH*, *espJ*, *espK*, and *pe35* in both, and, additionally, *ppe68* in *M. lepromatosis*. Of the remaining genes in this locus, *esxB*, *esxA*, and *espH* are the least conserved (69–73% protein identity) between *M. leprae* and *M. lepromatosis*, and a similar trend was observed for the unlinked *espACD* operon (*espA*, 78%; *espC*, 77%; and *espD*, 86% protein identity) that regulates the expression and secretion of EsxA in a mutually dependent manner in *M. tuberculosis* (43–45).

Of the four other T7Ss, ESX-2 and ESX-4 are predicted to be nonfunctional in *M. leprae* and *M. lepromatosis*, whereas the ESX-5 locus is highly conserved. However, compared with *M. tuberculosis*, only the ESX-5 core genes (*eccABCDE5* and *mycP5*) remain intact in both leprosy bacilli, there are no *esx* genes, and the PE protein gene (*ML2534c*/*MLPM_2534*) is nonfunctional. On the contrary, ESX-3 is the most conserved T7S

system in mycobacteria and seems to fulfill an essential function in metal homeostasis, although its role in virulence is less clear (45).

Neuropathogenesis. The ability to invade the Schwann cells of the peripheral nervous system is a hallmark of *M. leprae*, and this leads to the neuropathy and nerve damage associated with leprosy. Adherence to Schwann cells (46) has been proposed to be mediated by two cell wall components: the laminin-binding protein (ML1683c) and the terminal trisaccharide moiety of phenolic glycolipid 1 (PGL-1). To produce the trisaccharide, several enzymes are required, namely a rhamnosyl transferase (ML0128), a glucosyltransferase (ML2348), and four methyltransferases (ML0126, ML0127, ML23246c, and ML2347) (47). The genes encoding both these adhesin systems are highly conserved in *M. lepromatosis*, so invasion of Schwann cells is to be expected. Given the paucity of well-defined cases of infection with *M. lepromatosis*, studies of nerve involvement have not yet been conducted, but this will be facilitated by the tools arising from our investigation of the *M. lepromatosis* genome.

Disease Management and New Interventions. Until very recently, recognition of *M. lepromatosis* as a separate species was questioned. Currently, *M. lepromatosis* can be identified by a nested PCR technique that targets the 16S rDNA (22). Given the 98% identity of the *M. lepromatosis* and *M. leprae* 16S rDNA sequences, a possible source of confusion, it may be advisable to establish a new method of identification that exploits sequences confined to *M. lepromatosis* such as the species-specific PCR templates and primers described here (Table 1 and Table S4). Immunodiagnostic approaches for leprosy are being pursued by using the highly specific trisaccharide from PGL-1 and LID1 (48), a fusion protein that includes sequences from genes *ML0405* (*espA*) and *ML2331*. PGL-1-based tests should also detect *M. lepromatosis*, but tests involving LID-1 may be less sensitive because of the extensive variation in EspA reported earlier.

DLL cases resulting from infection with *M. lepromatosis* have responded favorably to the standard MDT (49), and, on examination of the drug resistance determining regions in the genes coding for the targets of rifampin, dapsone, and fluoroquinolones, only drug-susceptible sequences were found. New drugs developed to treat tuberculosis may also find application in leprosy. Inspection of the *M. lepromatosis* and *M. leprae* gene sequences for the targets of the experimental drugs bedaquiline, benzothiazinones, and Q203 suggest that these should be active, whereas the nitroimidazole prodrugs PA-824, TBA354, and delamanid will not be effective because the *ddn* gene, coding for the nitroreductase required for their activation, is missing.

Geographical Survey for *M. lepromatosis*. To gain more insight into the global distribution of *M. lepromatosis*, a differential PCR test was implemented by using species-specific primers targeting *hemN* and RLEP (*SI Materials and Methods*). A total of 227 specimens from patients with leprosy were chosen (Table 1),

Table 1. Geographical survey of leprosy bacilli by differential PCR analysis

| Country of origin	Sample size (suspicion of DLL/Lucio's)	M. lepromatosis	M. leprae
Venezuela	77	0	77
Mexico	64 (4)	6	58
Mali	48	0	48
Brazil	33	0	33
Others	5 (2)	0	5

PCR was performed using primers specific for each species: LPM244F and LPM44R for *M. lepromatosis*; RLEP-7 and RLEP-8 for *M. leprae*. Full details are provided in *SI Materials and Methods*.

including some with a history or suspicion of DLL or Lucio's reaction ($n = 6$). The largest patient groups were from Venezuela ($n = 77$), Mexico ($n = 64$), Mali ($n = 48$), and Brazil ($n = 33$); a small number of samples suspected of presenting with Lucio's reaction were obtained from elsewhere (Table 1). This analysis revealed the presence of *M. leprae* DNA in 221 cases and *M. lepromatosis* in only six, with no evidence for mixed infections. All six *M. lepromatosis* cases were of Mexican origin. Among the samples from DLL or Lucio's reaction cases, two were positive for *M. lepromatosis* and four for *M. leprae*.

On the Origin and Evolution of *M. lepromatosis*. The results from the genome-wide comparison of *M. leprae* and *M. lepromatosis* indicate that pseudogenization took place in their ancestral forms and that the MRCA itself likely had a genome of reduced size compared with all other known mycobacteria. Based on the rate of nonsynonymous substitution in pseudogenes, it was estimated that a single massive pseudogenization event took place approximately 20 Mya (50). Since their separation from the MRCA, deletions and more pseudogenes have appeared in both species. *M. lepromatosis* shares the same repeat families with *M. leprae*, including their genomic locations, but these have diverged extensively in sequence. In *M. leprae*, genome reduction and gene truncation have been attributed to recombinational events between different repeat copies, but these events likely occurred in the MRCA (17, 33).

To estimate the divergence times of *M. lepromatosis* and the currently available *M. leprae* strains, substitution rates were calculated in a Bayesian framework by using the software package BEAST (Bayesian Evolutionary Analysis Sampling Trees). For phylogenetic and divergence time analysis, the *M. lepromatosis* genome was aligned with 18 modern and ancient *M. leprae* genomes. On average, there were 90 nucleotide substitutions between two *M. leprae* strains and 275,518 substitutions between *M. leprae* and *M. lepromatosis*. A substitution rate of 7.67^{-9} substitutions per site per year was estimated (Fig. S2A), similar to previous estimates using *M. leprae* genomes only (20). The resulting divergence time from the MRCA (TMRCA) for all *M. leprae* strains was calculated as 3,607 y ago [2,204–5,525 y ago 95% highest probability density (HPD)], comparable to previous results (20) (Fig. S2B). The TMRCA for *M. leprae* and *M. lepromatosis* was estimated to be 13.9 Mya (8.2–21.4 Mya 95% HPD; Fig. S2C). In this respect, the two leprosy bacilli differ quite markedly from the species comprising the *M. tuberculosis* complex (MTBC), as, from a recent paleomicrobiogical investigation that used two independent dating approaches, it was concluded that the maximal TMRCA was <6,000 y for the MTBC (51).

A phylogenetic comparison by maximum parsimony of *M. lepromatosis* with various *M. leprae* strains of different geographic origins and SNP subtypes is shown in Fig. 4 and by neighbor joining in Fig. S3. To gain further insight into the phylogenetic placement of *M. lepromatosis* among other mycobacterial species, additional phylogenetic trees were generated based on the concatenated amino acid alignments of GyrB, RpoB, and RpoC (Fig. S4), as well as the alignments of the 16S genes (Fig. S5). In all four phylogenetic trees, *M. lepromatosis* is positioned between the mycobacteria used as outgroups and *M. leprae*. The *M. lepromatosis* branch is closest to the *M. leprae* SNP-type 3K strains, consistent with the very recent report of the 3K strains (branch 0) being the most ancestral lineage of *M. leprae* known to date (20). The geographic distribution of type 3K strains is diverse, but sampling is insufficiently broad to predict a tentative origin. On the contrary, the predominance of reported DLL and confirmed cases of infection with *M. lepromatosis* in Mexico suggest that this pathogen may have evolved in Central America. More extensive investigation is required to explore this possibility and to retrace its origin.
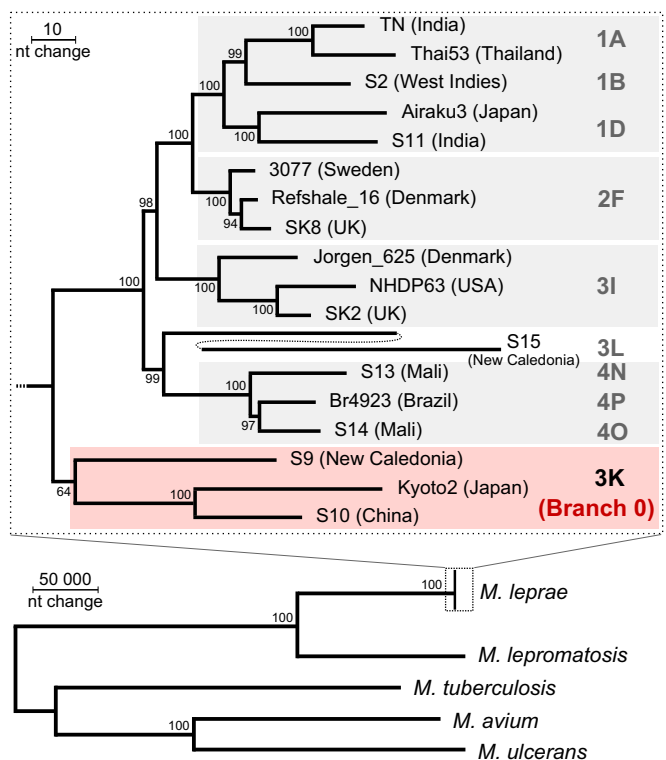
Fig. 4. Phylogeny of *M. lepromatosis* and *M. leprae* strains. Phylogenetic relationship of *M. lepromatosis* genome using a maximum parsimony tree, including *M. tuberculosis*, *M. avium*, and *M. ulcerans* as outgroups. SNP type is given at branch tips. Bootstrap support is indicated for each node. The long branch of S15 was split to reduce space.

Environmental Sources. *M. leprae* has long been considered an obligate human pathogen with its primary route of transmission being interhuman. In the past 30 y, the nine-banded armadillo has been identified as a natural reservoir of *M. leprae* in the southern United States, and evidence for zoonotic transmission to humans is accumulating (34). The existence of nonhuman hosts or natural reservoirs of *M. lepromatosis* has not yet been investigated, but, recently, an apparent outbreak of *M. lepromatosis* infection in red squirrels (*Sciurus vulgaris*) was reported in the United Kingdom (52). Examination of infected squirrel tissue using the PCR-based sequencing procedures for the *hemN* gene outlined here has confirmed this finding and thus provides evidence for a nonhuman reservoir or intermediate host for *M. lepromatosis*. To date, the most convincing human cases of *M. lepromatosis* infection, particularly those with DLL, came from Mexico. One of the regional culinary traditions in rural Mexico is consumption of field rats (*Rattus rattus*) (53). Because *M. lepromatosis* seems to naturally infect rodents, such as squirrels, it is conceivable that field rats are a host and may serve as a disease reservoir. When a retrospective survey of confirmed cases of *M. lepromatosis* was conducted, two of the six Mexican subjects admitted having consumed meat from field rats. Availability of the *M. lepromatosis* genome sequence will enable us to search systematically for its presence in other potential animal reservoirs as well as in extant cases of leprosy. As a result, deeper understanding will be obtained of the incidence, etiology, epidemiology, clinical features, and pathogenesis of leprosy caused by *M. lepromatosis*.

Materials and Methods

DNA Extraction and Sequencing. DNA was extracted from the biopsy specimen Mx1-22A (32), and the Illumina library was prepared as described elsewhere (20). To overcome the problem of the high level of host DNA in the library,

MICROBIOLOGY

we used two methods for enrichment of *M. lepromatosis* DNA: (*i*) whole-genome array capture using an *M. leprae* tiling array (20) and (*ii*) removal of human DNA by hybridization with a human genomic DNA bait library.

Genome Assembly and Annotation. Reads mapping to the human genome were discarded and duplicate reads were removed before the assembly. De novo genome assembly was done in MIRA version 4.0rc4 (54). Contigs were anchored to the *M. leprae* TN genome, and those contigs that did not match were screened for contaminants and the presence of mycobacterial genes. Genome sequence synteny between *M. lepromatosis* and *M. leprae* was visualized in ACT (Artemis Comparison Tool) (55) (Fig. 1).

PCR Procedures. To confirm the presence of the *hemN* gene and its flanking sequence, including a genomic rearrangement, we designed PCR primers

(Table S4) to amplify overlapping genomic targets. Details of the procedures used for the geographical survey are provided in *SI Materials and Methods*.

SNP Calling and Phylogeny. Genome sequences of *Mycobacterium avium* K10, *M. lepromatosis*, and the published *M. leprae* strains were aligned against the *M. leprae* TN genome. SNP alignments were analyzed in MEGA6 (Molecular Evolutionary Genetics Analysis version 6.0) (56). Further details of bioinformatics procedures, Bayesian dating analysis, and phylogeny are provided in *SI Materials and Methods*.

1. World Health Organization (2013) Global leprosy: Update on the 2012 situation. *Wkly Epidemiol Rec* 88(35):365–379.
2. Ridley DS, Jopling WH (1966) Classification of leprosy according to immunity. A five-group system. *Int J Lepr Other Mycobact Dis* 34(3):255–273.
3. Britton WJ, Lockwood DN (2004) Leprosy. *Lancet* 363(9416):1209–1219.
4. Scollard DM, et al. (2006) The continuing challenges of leprosy. *Clin Microbiol Rev* 19(2):338–381.
5. Lucio R, Alsarado Y (1852) *Opusculo sobre el mal de San Làzaro, ó elefanciasis de los griegos, escrito por los profesores de medicina y cirugia* (Imprento de M. Murguia y Compañia, Mexico City, Mexico).
6. Latapi F, Chevez-Zamora A (1948) The "spotted" leprosy of Lucio: An introduction to its clinical and histological study. *Int J Lepr* 16:421–437.
7. Rea TH (1979) Lucio's phenomenon: An overview. *Lepr Rev* 50(2):107–112.
8. Rea TH, Jerskey RS (2005) Clinical and histologic variations among thirty patients with Lucio's phenomenon and pure and primitive diffuse lepromatosis (Latapi's lepromatosis). *Int J Lepr Other Mycobact Dis* 73(3):169–188.
9. Moschella SL (1967) The lepra reaction with necrotizing skin lesions. A report of six cases. *Arch Dermatol* 95(6):565–575.
10. Romero A, Brenes, Ibarra A, Fallas M (1949) Clinical study of lepromatous leprosy in Costa Rica. *Int J Lepr* 17(1-2):27–33.
11. Vargas-Ocampo F (2007) Diffuse leprosy of Lucio and Latapí: A histologic study. *Lepr Rev* 78(3):248–260.
12. Sehgal VN (2005) Lucio's phenomenon/erythema necroticans. *Int J Dermatol* 44(7):602–605.
13. Ang P, Tay Y-K, Ng S-K, Seow C-S (2003) Fatal Lucio's phenomenon in 2 patients with previously undiagnosed leprosy. *J Am Acad Dermatol* 48(6):958–961.
14. Peixoto AB, Portela PS, Leal FRP de C, Brotas AM, Rodrigues NC dos S (2013) Lucio's phenomenon. Case study of an exceptional response to treatment exclusively with multibacillary multidrug therapy. *An Bras Dermatol* 88(6, Suppl 1):93–96.
15. World Health Organization (2014) WHO Recommended MDT Regimens. Available at www.who.int/lep/mdt/regimens/en/. Accessed September 24, 2014.
16. Helmer KA, Fleischfresser I, Kucharski-Esmanhoto LD, Fillus Neto J, Santamaria JR (2004) The Lucio's phenomenon (necrotizing erythema) in pregnancy. *An Bras Dermatol* 79(2):205–210.
17. Cole ST, et al. (2001) Massive gene decay in the leprosy bacillus. *Nature* 409(6823):1007–1011.
18. Williams DL, Gillis TP, Portaels F (1990) Geographically distinct isolates of Mycobacterium leprae exhibit no genotypic diversity by restriction fragment-length polymorphism analysis. *Mol Microbiol* 4(10):1653–1659.
19. Monot M, et al. (2009) Comparative genomic and phylogeographic analysis of Mycobacterium leprae. *Nat Genet* 41(12):1282–1289.
20. Schuenemann VJ, et al. (2013) Genome-wide comparison of medieval and modern Mycobacterium leprae. *Science* 341(6142):179–183.
21. Han XY, et al. (2008) A new Mycobacterium species causing diffuse lepromatous leprosy. *Am J Clin Pathol* 130(6):856–864.
22. Han XY, Sizer KC, Velarde-Félix JS, Frias-Castro LO, Vargas-Ocampo F (2012) The leprosy agents Mycobacterium lepromatosis and Mycobacterium leprae in Mexico. *Int J Dermatol* 51(8):952–959.
23. Han XY, Sizer KC, Tan H-H (2012) Identification of the leprosy agent Mycobacterium lepromatosis in Singapore. *J Drugs Dermatol* 11(2):168–172.
24. Jessamine PG, et al. (2012) Leprosy-like illness in a patient with Mycobacterium lepromatosis from Ontario, Canada. *J Drugs Dermatol* 11(2):229–233.
25. Monteiro R, et al. (2012) Lucio's phenomenon: Another case reported in Brazil. *An Bras Dermatol* 87(2):296–300.
26. Souza CS, Roselino AM, Figueiredo F, Foss NT (2000) Lucio's phenomenon: Clinical and therapeutic aspects. *Int J Lepr Other Mycobact Dis* 68(4):417–425.
27. Saoji V, Salodkar A (2001) Lucio leprosy with lucio phenomenon. *Indian J Lepr* 73(3):267–272.
28. Thappa DM, Karthikeyan K, Kumar BJ (2002) Is it Lucio leprosy with Lucio phenomenon or something else? *Indian J Lepr* 74(2):161–166.
29. Kumari R, Thappa DM, Basu D (2008) A fatal case of Lucio phenomenon from India. *Dermatol Online J* 14(2):10.
30. Golchai J, Zargari O, Maboodi A, Maboodi A, Granmayeh S (2004) Lepromatous leprosy with extensive unusual ulcerations and cachexia. Is it the first case of Lucio's phenomenon from Iran? *Int J Lepr Other Mycobact Dis* 72(1):56–59.
31. Choon SE, Tey KE (2009) Lucio's phenomenon: A report of three cases seen in Johor, Malaysia. *Int J Dermatol* 48(9):984–988.
32. Vera-Cabrera L, et al. (2011) Case of diffuse lepromatous leprosy associated with "Mycobacterium lepromatosis". *J Clin Microbiol* 49(12):4366–4368.
33. Cole ST, Supply P, Honoré N (2001) Repetitive sequences in Mycobacterium leprae and their impact on genome plasticity. *Lepr Rev* 72(4):449–461.
34. Truman RW, et al. (2011) Probable zoonotic leprosy in the southern United States. *N Engl J Med* 364(17):1626–1633.
35. Stinear TP, et al. (2007) Reductive evolution and niche adaptation inferred from the genome of Mycobacterium ulcerans, the causative agent of Buruli ulcer. *Genome Res* 17(2):192–200.
36. Demangel C, Stinear TP, Cole ST (2009) Buruli ulcer: Reductive evolution enhances pathogenicity of Mycobacterium ulcerans. *Nat Rev Microbiol* 7(1):50–60.
37. Chu BC, et al. (2010) Siderophore uptake in bacteria and the battle for iron with the host; a bird's eye view. *Biometals* 23(4):601–611.
38. Braun V, Hantke K (2011) Recent insights into iron import by bacteria. *Curr Opin Chem Biol* 15(2):328–334.
39. De Voss JJ, et al. (2000) The salicylate-derived mycobactin siderophores of Mycobacterium tuberculosis are essential for growth in macrophages. *Proc Natl Acad Sci USA* 97(3):1252–1257.
40. Reddy PV, et al. (2013) Disruption of mycobactin biosynthesis leads to attenuation of Mycobacterium tuberculosis for growth and virulence. *J Infect Dis* 208(8):1255–1265.
41. Kai M, et al. (2013) Characteristic mutations found in the ML0411 gene of Mycobacterium leprae isolated in Northeast Asian countries. *Infect Genet Evol* 19:200–204.
42. Simeone R, et al. (2012) Phagosomal rupture by Mycobacterium tuberculosis results in toxicity and host cell death. *PLoS Pathog* 8(2):e1002507.
43. Fortune SM, et al. (2005) Mutually dependent secretion of proteins required for mycobacterial virulence. *Proc Natl Acad Sci USA* 102(30):10676–10681.
44. Garces A, et al. (2010) EspA acts as a critical mediator of ESX1-dependent virulence in Mycobacterium tuberculosis by affecting bacterial cell wall integrity. *PLoS Pathog* 6(6):e1000957.
45. Stoop EJM, et al. (2011) Zebrafish embryo screen for mycobacterial genes involved in the initiation of granuloma formation reveals a newly identified ESX-1 component. *Dis Model Mech* 4(4):526–536.
46. Rambukkana A (2001) Molecular basis for the peripheral nerve predilection of Mycobacterium leprae. *Curr Opin Microbiol* 4(1):21–27.
47. Tabouret G, et al. (2010) Mycobacterium leprae phenolglycolipid-1 expressed by engineered M. bovis BCG modulates early interaction with human phagocytes. *PLoS Pathog* 6(10):e1001159.
48. de Souza MM, Netto EM, Nakatani M, Duthie MS (2014) Utility of recombinant proteins LID-1 and PADL in screening for Mycobacterium leprae infection and leprosy. *Trans R Soc Trop Med Hyg* 108(8):495–501.
49. Han XY, Jessurun J (2013) Severe leprosy reactions due to Mycobacterium lepromatosis. *Am J Med Sci* 345(1):65–69.
50. Han XY, et al. (2009) Comparative sequence analysis of Mycobacterium leprae and the new leprosy-causing Mycobacterium lepromatosis. *J Bacteriol* 191(19):6067–6074.
51. Bos KI, et al. (2014) Pre-Columbian mycobacterial genomes reveal seals as a source of New World human tuberculosis. *Nature* 514(7523):494–497.
52. Meredith A, et al. (2014) Leprosy in red squirrels in Scotland. *Vet Rec* 175(11):285–286.
53. Chacon R (October 8, 1999) In Mexico, field rats are secret delicacy. *Miami Herald*. Available at www.latinamericanstudies.org/mexico/rats.htm. Accessed October 16, 2014.
54. Chevreux B, Wetter T, Suhai S (1999) Genome sequence assembly using trace signals and additional sequence information. *Computer Science and Biology: Proceedings of the German Conference on Bioinformatics (GCB)*, Vol 99, pp 45–56. Available at www.bioinfo.de/isb/gcb99/talks/chevreux/main.html.
55. Carver TJ, et al. (2005) ACT: The Artemis Comparison Tool. *Bioinformatics* 21(16):3422–3423.
56. Tamura K, Stecher G, Peterson D, Filipski A, Kumar S (2013) MEGA6: Molecular Evolutionary Genetics Analysis version 6.0. *Mol Biol Evol* 30(12):2725–2729.